J. Fluid Mech. (1993), *vol.* 252, *pp.* 383–398

Effect of wind profile on the instability of wind blowing over water†

By L. C. MORLAND[1] AND P. G. SAFFMAN[2]

[1] Department of Mathematics, Southern Methodist University, Dallas, TX 75275, USA

[2] Department of Applied Mathematics, California Institute of Technology, Pasadena, CA 91125, USA

(Received 6 August 1991 and in revised form 4 January 1993)

A linear stability analysis of the inviscid, parallel flow of air over water leads to an eigenvalue problem for the wave speed, which is solved numerically for air profiles typical of both laminar and turbulent flows. Comparison is made with Miles' (1957) theory; growth rates differ from those predicted from the Miles (1957) formula but are in agreement with Conte & Miles' (1959) computations for turbulent flow profiles. In the limit of a highly sheared wind profile the numerical computations retrieve the Kelvin–Helmholtz instability.

1. Introduction

Miles (1957) described a quasi-steady mechanism by which a parallel, sheared, inviscid air flow could amplify water waves. His analysis led to a boundary value problem for the perturbation stream function and a formula for the growth rate. An approximate solution to the boundary value problem was used to write the growth rate in terms of wavelength and wind velocity profile. The formula is valid for a wave that is sufficiently long that the associated critical layer in the air lies above the viscous sublayer adjoining the water surface. A physical interpretation was given by Lighthill (1962) in which it was demonstrated that a perturbation to a parallel air flow due to the presence of a water wave could grow in the neighbourhood of the critical layer, leading to growth of the wave. Conte & Miles (1959) solved the boundary value problem for the perturbation stream function numerically, and Miles (1959) states that the numerical growth rates are somewhat smaller than those calculated from his formula. Miles' theory of water-wave generation has played a central role in much of the subsequent theoretical and experimental work on the formation of water waves by wind.

Following the work of Benjamin (1959) on shearing flow over a wavy boundary, Miles (1962*b*) incorporated a viscous boundary layer in the air at the water surface, thus extending his theory to include shorter waves for which the critical layer lies in the viscous sublayer; with this modification the wave generation mechanism is commonly refered to as the 'Miles–Benjamin' mechanism. Subsequent papers concerning the viscous theory include those of Valenzuela (1976) who studied the growth of capillary–gravity waves by solving the Orr–Sommerfield equation numerically for a coupled air–water flow, and van Gastel, Janssen & Kamen (1985) who re-derived the Miles–Benjamin theory using asymptotic expansions. This theory has been used for comparison with experiments in which the waves generated have lengths of a few

† With an Appendix by J. W. Miles

centimetres, for example the wind-wave tunnel experimental work of Kahma & Donelan (1988).

Akylas (1982) examined direct resonance between the weakly unstable water modes predicted by the Miles theory and Tollmien–Schlichting waves in the air, the occurrence of which had first been demonstrated by Miles (1962*b*). For an air flow of Blasius boundary-layer type he demonstrated that direct resonance can occur for waves of length greater than 12 cm and provides a mechanism for the rapid amplification of such waves.

Field work performed to examine the validity of the Miles (1957) mechanism includes Snyder & Cox (1966), Barnett & Wilkerson (1967), Dobson (1971), Elliott (1972), Snyder (1974) and Snyder *et al.* (1981). The observed growth rates were compared with the numerical results of Conte & Miles and the results of the further computations performed by Long (1980). With the exception of Snyder & Cox and Barnett & Wilkerson, these investigations involved making measurements of wave-induced pressure fluctuations above the water surface. Snyder & Cox and Barnett & Wilkerson measured the growth in height of waves, the former using a wave recorder towed by a boat and the latter using airborne radar measurements. The three earliest investigations found growth rates that exceeded those predicted from the Miles theory by a factor of between five and eight. Elliott and Snyder found growth rates that were much closer to those predicted by Miles, although Elliott's growth rates exceeded those of Snyder by a factor of two.

The discrepancies between the results of previous investigations and the difficulties associated with making measurements at sea led Snyder *et al.* to re-examine the methods by which pressure fluctuations were measured in the previous three studies and to make new measurements. They were able to reconcile the differences between the results of Elliott and Snyder and found the re-analysed results to be in agreement with their new data. These three consistent sets of results were found to be in reasonable agreement with the Miles theory. They were unable to explain the disagreement with Dobson's results and the measurements made by monitoring wave heights. The results of a field investigation at sea by Hasselman & Bösenberg (1991) are also consistent with those of Snyder *et al.*

Miles' theory does not include the influence of turbulence in the air on the growth of waves apart from the use of logarithmic-type profiles for the wind. This deficiency has been addressed by several authors who have incorporated a turbulence model into their analysis. Van Duin & Janssen (1992) describe some of this work in an investigation of dependence of growth rates on model type. They note that until their study the Miles theory has shown better agreement with observed growth rates than the predictions of theories that include a turbulence model. They also comment that for long waves the observed growth rates of Snyder *et al.* exceed those of the Miles theory by a factor of two, but cite the work of Makin (1988) who claims that the experimental work may overestimate growth rates by a factor of two. These remarks appear to support the agreement between the Miles theory and the observed growth rates of Snyder *et al.*, but also demonstrate the uncertainty involved in measuring growth rates.

The purpose of the present investigation is to re-examine the inviscid flow of air over water as a problem in hydrodynamic stability and to compare the results of a numerical solution of the resulting eigenvalue problem with the Miles (1957) formula, given by equation (2.10). We consider the stability of a basic state in which the water is stagnant and the wind speed increases monotonically from zero with height above the water surface. Two distinct types of air velocity profile are examined: exponential profiles that are representative of laminar flow and logarithmic profiles that are a more realistic

approximation to the mean flow of a turbulent wind. The condition that the critical layer should lie above the viscous sublayer limits the applicability of inviscid theory to gravity waves and so inviscid theory is more relevant to field experiments than laboratory investigations.

Agreement between growth rates calculated from the Miles formula and from the numerics is found to be poor for the laminar-type profiles, but this is not surprising since we find that growth rates computed by either method depend sensitively on the wind profile. For the logarithmic profiles there is good qualitative agreement but we find that the Miles formula overestimates the numerical growth rates by a factor of approximately two. In contrast, we find good agreement between our results and the results presented by Conte & Miles (1959) in their table 1.

In the limit of a highly sheared exponential-type profile we find that the Kelvin–Helmholtz instability of a vortex sheet is retrieved. This is of mathematical rather than physical interest since the Kelvin–Helmholtz instability manifests itself at short wavelengths at which inviscid theory is not valid.

Shemdin (1972) performed a numerical investigation of waves on an inviscid coupled air–water flow, when there is also a current in the water, with the aim of examining the effect of the current on the phase velocity of water waves, but he did not consider the occurrence of unstable modes. Shemdin found that surface drift increases the phase velocity of waves that are travelling in the direction of the drift, but that the effect was limited by the drift being at most 4% of the wind speed. For the long waves to which inviscid theory is applicable this correction is negligible, so in our investigation, consistent with Miles (1957), we have not included a current in the water. Similarly, surface tension at the water surface has not been included.

An important result in the theory of inviscid channel flow is Howard's (1961) semicircle theorem which restricts wave speeds c, with positive imaginary part, to lie in the semicircle in the upper half-c-plane with origin $\frac{1}{2}(U_{\min}+U_{\max})$ and radius $\frac{1}{2}(U_{\max}-U_{\min})$. $U_{\min}$ and $U_{\max}$ are the minimum and maximum velocity respectively of the basic parallel flow. The theorem was originally proved for channel flows and was extended to a flow with a free surface by Yih (1972). In Appendix A we show that the theorem can be further extended to include coupled free-surface flows of the type being examined here. When the wind speed is unbounded, as it is for logarithmic-type profiles, the analysis proceeds as far as the conclusion below equation (A 3), which is that a necessary condition for instability is that the phase velocity is greater than $U_{\min}$.

Another important result is Squire's theorem for an inviscid fluid. The theorem, described for the case of channel flow by Drazin & Reid (1981), states that to every unstable three-dimensional disturbance of an ideal fluid in parallel flow there corresponds a more unstable two-dimensional disturbance that can be found by means of Squire's transformation (Squire 1933). Morland, Saffman & Yuen (1991) extended the transformation and theorem to include a flow with a free surface, and the further extension of the transformation to the coupled free-surface flow considered here follows in a straightforward manner. However, the theorem can only be extended to include the laminar profiles and not the logarithmic profiles. The details are described in the Appendix.

2. Mathematical formulation

The basic flow consists of a semi-infinite, parallel flow of air above a semi-infinite stagnant body of water. The interface between the two fluids is a free surface which in the basic flow is planar, and across which fluid velocity is continuous. Our numerical

results are limited to the case when there is no current in the water, consistent with the problem analysed by Miles. A consequence of Squire's transformation is that only two-dimensional disturbances to the basic state need be computed.

Cartesian coordinates are defined with origin at the undisturbed interface, x-axis parallel to the interface and y-axis vertically upwards into the air. The fluids have velocity $\boldsymbol{u} = (u, v)$ and pressure p, with appropriate subscripts when it is necessary to distinguish between air and water. The interface is given by $y = \eta(x, t)$. The fluid motion in both fluids is governed by the Euler equations and the equation of continuity,

$$\boldsymbol{u}_t + \boldsymbol{u}\cdot\boldsymbol{\nabla}\boldsymbol{u} = -\boldsymbol{\nabla}p/\rho + \boldsymbol{g}, \tag{2.1a}$$

$$\boldsymbol{\nabla}\cdot\boldsymbol{u} = \boldsymbol{0}, \tag{2.1b}$$

where the acceleration due to gravity, $\boldsymbol{g}$, acts in the negative y-direction.

At the free surface continuity of pressure is applied,

$$[p]^{\mathrm{a}}_{\mathrm{w}} = 0 \quad \text{on} \quad y = \eta, \tag{2.2a}$$

where indices a and w denote air and water respectively. The condition that the interface is a material surface of both fluids requires

$$\eta_t + \boldsymbol{u}\cdot\boldsymbol{\nabla}\eta - v = 0 \quad \text{on} \quad y = \eta \tag{2.2b}$$

to be applied for both fluids. At large distances from the interface the fluid velocity must tend to that of the basic state.

With small time-dependent two-dimensional perturbations, the velocity and pressure are $\boldsymbol{u} = (U+u', v'), p = -\rho g y + p'$ and the free surface is $y = \eta'$. Neglecting products of small quantities in (2.1), (2.2) and applying the boundary condition at infinity gives the linearized equations

$$u'_t + Uu'_x + U_y v' = -p'_x/\rho, \tag{2.3a}$$

$$v'_t + Uv'_x = -p'_y/\rho, \tag{2.3b}$$

$$u'_x + v'_y = 0 \tag{2.3c}$$

in the fluids, and

$$\eta'_t + U\eta'_x - v' = 0 \quad \text{on} \quad y = 0, \tag{2.3d}$$

$$[p']^{\mathrm{a}}_{\mathrm{w}} = (\rho_{\mathrm{a}} - \rho_{\mathrm{w}})\, g\eta' \quad \text{on} \quad y = 0, \tag{2.3e}$$

$$(u', v') \to 0 \quad \text{as} \quad y \to \pm\infty, \tag{2.3f}$$

where (2.3d) is applied for both air and water. We seek normal mode solutions of the form $u' = \phi_y(y)\, \mathrm{e}^{\mathrm{i}(kx-\sigma t)}$, $v' = -\mathrm{i}k\phi(y)\, \mathrm{e}^{\mathrm{i}(kx-\sigma t)}$ and $\eta' = a\, \mathrm{e}^{\mathrm{i}(kx-\sigma t)}$, where k is the streamwise wavenumber and σ is the angular frequency, possibly complex. To obtain physical quantities the real parts of the above expressions are to be taken; ϕ is in general complex valued. Eliminating the pressure between (2.3a) and (2.3b) gives Rayleigh's equation

$$\phi_{yy} - \left(k^2 + \frac{U_{yy}}{U-c}\right)\phi = 0, \tag{2.4a}$$

where $c = \sigma/k$ is the wave speed and the equation applies in both fluids. Equation (2.3d) gives $\phi_{\mathrm{a}}(0) = \phi_{\mathrm{w}}(0) = a(c - U(0))$. When these relationships are used to eliminate a, and the normal mode form of the solution is substituted, (2.3e) becomes

$$[\rho((U-c)^2\phi_y - (U_y(U-c) + g)\,\phi)]^{\mathrm{a}}_{\mathrm{w}} = 0 \quad \text{on} \quad y = 0. \tag{2.4b}$$

The boundary condition at infinity, (2.3f), requires that

$$\phi \to 0 \quad \text{as} \quad y \to \pm\infty. \tag{2.4c}$$

For laminar-type profiles the flow in the air is taken to be characterized by two parameters: the air velocity at large height above the water surface, U_∞, and a measure of the height to which vorticity has penetrated from the water surface, Δ, defined by

$$\Delta = \frac{2}{U_\infty}\int_0^\infty y U_y(y)\,\mathrm{d}y, \tag{2.5}$$

i.e. twice the height of the vorticity centroid. Two families of profiles are examined: the exponential profiles defined by

$$U(y) = U_\infty(1-\mathrm{e}^{-2y/\Delta}), \quad 0 < y < \infty, \tag{2.6a}$$

and the error function profiles defined by

$$U(y) = U_\infty \operatorname{erf}\left(\frac{2y}{\pi^{\frac{1}{2}}\Delta}\right), \quad 0 < y < \infty. \tag{2.6b}$$

The error function profiles arise when viscous air is started impulsively into motion with uniform velocity U_∞ from rest. The vorticity-layer thickness then evolves in time as $\Delta = 4(\nu_a t/\pi)^{\frac{1}{2}}$. The exponential profiles are similar in shape to the error function profiles and have the convenient features that they allow Rayleigh's equation to be integrated analytically (see Appendix B by Miles) and the integral in Miles' formula for the growth rate to be evaluated exactly. When velocities are scaled with U_∞ and lengths with U_∞^2/g the profiles depend on the single non-dimensional parameter $\Delta g/U_\infty^2$.

The profiles taken to be representative of turbulent boundary layer flow are the 'lin-log' profiles which consist of a linear profile in a viscous sublayer that merges smoothly with a logarithmic velocity profile in a constant-stress region above. In the next section we present results for the following profile:

$$U(y) = \begin{cases} u_*^2 y/\nu, & y < y_1 \\ (u_*/\kappa)(\sinh^{-1}(\kappa u_*(y-y_1)/\nu) + A - \log(2\kappa)), & y \geqslant y_1, \end{cases} \tag{2.7a}$$

where ν is the kinematic viscosity of air, u_* is the friction velocity, κ is von Kármán's constant, A is the roughness constant and y_1 is the transition height between the linear and logarithmic sections of the profile. For large y, $U(y) \sim (u_*/\kappa)(\log(u_* y/\nu) + A)$. In our calculation we take $\kappa = 0.41$, and in the results presented $A = 2.3$, which is a suitable value for flow over a smooth surface (Townsend 1976). We have also obtained some results for smaller values of A as a way of examining the influence of a water surface that has been roughened by the development of waves. The requirement that the profile is continuous at $y = y_1$ determines that $u_* y_1/\nu = (A - \log(2\kappa))/\kappa \approx 6.1$, which is within the accepted range of values for the viscous sublayer height.

We have also examined the 'lin-log' profile described in Miles (1962*a*) and Valenzuela (1976) which is given by

$$U(y) = \begin{cases} u_*^2 y/\nu, & y < y_1 \\ u_*^2 y_1/\nu + (u_*/\kappa)(\alpha - \tanh(\frac{1}{2}\alpha)), & y \geqslant y_1, \end{cases} \tag{2.7b}$$

where α is defined by $\sinh(\alpha) = 2u_*\kappa(y-y_1)/\nu$, and we take $u_* y_1/\nu$ to be approximately 6.8 so that the large-y behaviour is the same as for the other lin-log profile. A purely logarithmic profile defined by

$$U(y) = (u_*/\kappa)(\log(u_* y/\nu + 1/\kappa) + A), \quad y \geqslant 0, \tag{2.7c}$$

has also been used. This profile has the appropriate behaviour at infinity and the

correct gradient at the water surface but has no viscous sublayer resulting in a vortex sheet at the water survace. All three profiles give similar results in the long-wave regime for which inviscid theory is valid.

For the purposes of computation we define the wind speed by $U_\infty = 20u_*$ and use the same scaling scheme as for the exponential-type profiles, which gives $g\nu/U_\infty^3$ as the dimensionless profile parameter. However, we present the results in dimensional variables.

Since $U \equiv 0$ in the water the solution of (2.4a) satisfying (2.4c) is $\phi_w = A\,e^{ky}$, where A is an arbitrary constant. Substituting for ϕ_w in (2.4) and scaling lengths with U_∞^2/g and velocities with U_∞ gives

$$\phi_{yy} - \left(k^2 + \frac{U_{yy}}{U-c}\right)\phi = 0, \quad 0 < y < \infty, \tag{2.8a}$$

$$sc^2\phi_y + (s(U_y c - 1) + 1 - c^2 k)\,\phi = 0 \quad \text{on} \quad y = 0, \tag{2.8b}$$

$$\phi \to 0 \quad \text{as} \quad y \to \infty, \tag{2.8c}$$

where $s = \rho_a/\rho_w$, and all variables in (2.8) are non-dimensional.

Equations (2.8) form an eigenvalue problem for the wave speed c and the eigenfunction $\phi(y)$. After the scaling described above, the non-dimensional wave speed is found to be a function of the non-dimensional wavelength, the density ratio of air to water s, and the profile parameter ($\Delta g/U_\infty^2$ in the case of the laminar profiles and $g\nu/U_\infty^3$ for the turbulent profiles). We fix the density ratio as 10^{-3} in all the computations. Numerical solution of the eigenvalue problem is performed by the iterative method described by Morland *et al*; a two-point boundary value problem consisting of (2.8a), (2.8b) and a normalization condition $\phi'(0) = 1$ is solved at each step of an application of the secant method to (2.8b). The two-point boundary value problem is solved by a shooting method.

Since the semicircle theorem qualitatively delineates the regions where the wave speed is complex, the calculations are unaffected by the existence of a critical layer for the transition wavelengths, except in so far that fine resolution is required near the value of y for which $U(y) = \mathrm{Re}\,(c)$, when $\mathrm{Im}\,(c)$ is small.

Solutions to the eigenvalue problem given in (2.8) will be compared with the results of Miles' analysis. He expressed the wave speed as

$$c = c_w(1 + 0.5s(\alpha + i\beta)(U_1/c_w)^2), \tag{2.9}$$

where $c_w = (g/k)^{\frac{1}{2}}$ is the phase velocity of water waves when $\rho_a = 0$ and U_1 is a reference velocity for the air. The influence of the air flow on the water waves is contained in the quantities α and β. Since $s \ll 1$ the correction to the phase velocity due to the air flow is small and Miles concentrated on finding β, for which he derived the formula

$$\beta = -\pi \frac{w_c''}{w_c'^3}\left(\int_{\xi_c}^{\infty} e^{-\xi} w^2\,d\xi\right)^2, \tag{2.10}$$

where $\xi = ky$, $w(\xi) = (U - c_w)/U_1$ and a prime denotes differentiation with respect to ξ. A subscript c indicates evaluation at the critical layer $\xi_c = ky_c$, which for a given profile and wavelength is defined by $U(y_c) = c_w$. If c_w does not lie between the maximum and minimum values of $U(y)$ then β is defined to be zero. From (2.9) the growth rate is given by $\sigma_i = 0.5sk\beta U_1^2/c_w$. In the case of the exponential profiles described by (2.6a) the expression for β, (2.10), can be evaluated to yield

$$\sigma_i = \frac{16\pi s k^2 \Delta U_\infty^2}{c_w(2+k\Delta)^2(4+k\Delta)^2}\left(1 - \frac{c_w}{U_\infty}\right)^{2+k\Delta}. \tag{2.11}$$

3. Results and discussion

If there is no current in the air, i.e. $U \equiv 0$, it is well known that for a given wavelength there are two distinct gravity waves with wave speed $\pm c_0$, where c_0 is given by

$$c_0 = \left(\frac{(\rho_w - \rho_a)\, g}{(\rho_w + \rho_a)\, k}\right)^{\frac{1}{2}}. \tag{3.1}$$

When there is a current in the air of the types considered in this paper we have found only two solutions at a given wavelength and these correspond to the gravity waves in the case of otherwise still air. The phase velocities are approximately $\pm c_0$; advection of the waves by the wind is very limited since the density of air is very small compared with that of water. This approximation remains valid unless the profile is highly sheared, in which case the Kelvin–Helmholtz instability manifests itself. This point is discussed further below.

The semicircle theorem dictates that the phase velocity of an unstable mode must lie in the range of U, which corresponds to the condition for instability in the Miles theory that c_w must lie in the range of U. Our numerical results indicate that advection by the wind of the wave with phase velocity of approximately $-c_0$ is never strong enough for the true velocity to be positive, and hence this mode is always stable. We find that the mode with positive phase velocity is unstable whenever its phase velocity lies in the range of U, consistent with the Miles theory.

For the exponential-type profiles when $\Delta g/U_\infty^2 = 0$ the air flow is a uniform stream and the interface is a vortex sheet. In this case the instability mechanism is the Kelvin–Helmholtz instability, an account of which can be found in Chandresakhar (1970), and for which the dispersion relation is

$$c = \frac{sU_\infty}{1+s} \pm \left(c_0^2 - \frac{sU_\infty^2}{(1+s)^2}\right)^{\frac{1}{2}}. \tag{3.2}$$

As $\Delta g/U_\infty^2 \to 0$ with $\lambda \gg \Delta$, where $\lambda = 2\pi/k$ is the wavelength, the numerical computations retrieve the Kelvin–Helmholtz instability. In this limit the approximation $\mathrm{Re}\,(c) \approx c_w$ becomes invalid for the unstable modes since from (3.2) their phase velocity is approximately constant, with value $sU_\infty/(1+s)$. The Kelvin–Helmholtz instability becomes significant in the instability of a smooth profile when Δ is small enough that waves that are long compared with Δ are Kelvin–Helmholtz unstable. From (3.2) and (3.1) modes are Kelvin–Helmholtz unstable when $\lambda g/U_\infty^2 < 2\pi s/(1-s^2)$ and hence the Kelvin–Helmholtz instability influences smooth profiles when $\Delta g/U_\infty^2 \ll 2\pi s/(1-s^2)$.

Figure 1(*a*, *b*) shows the growth rate against the phase velocity computed numerically and from the Miles formula for the exponential and error function profiles with $\Delta g/U_\infty^2 = 0.1$ and $\Delta g/U_\infty^2 = 0.01$. These values of $\Delta g/U_\infty^2$ fall out of the Kelvin–Helmholtz regime so that the wavelength can be retrieved approximately from $\mathrm{Re}\,(c) = c_w$. The figures show the sensitive dependence of growth rates on profile exhibited by both methods of computation; a factor of ten difference in $\Delta g/U_\infty^2$ produces a factor of approximately one hundred difference in growth rates. Also, despite the similarity between the two profile types, the figures show that at these values of $\Delta g/U_\infty^2$ the Miles formula produces larger growth rates than the numerics for the exponential profile and smaller growth rates for the error function profile.

We find that the relative size of the maximum growth rates predicted by the two methods of computation varies significantly with $\Delta g/U_\infty^2$. For example, for the

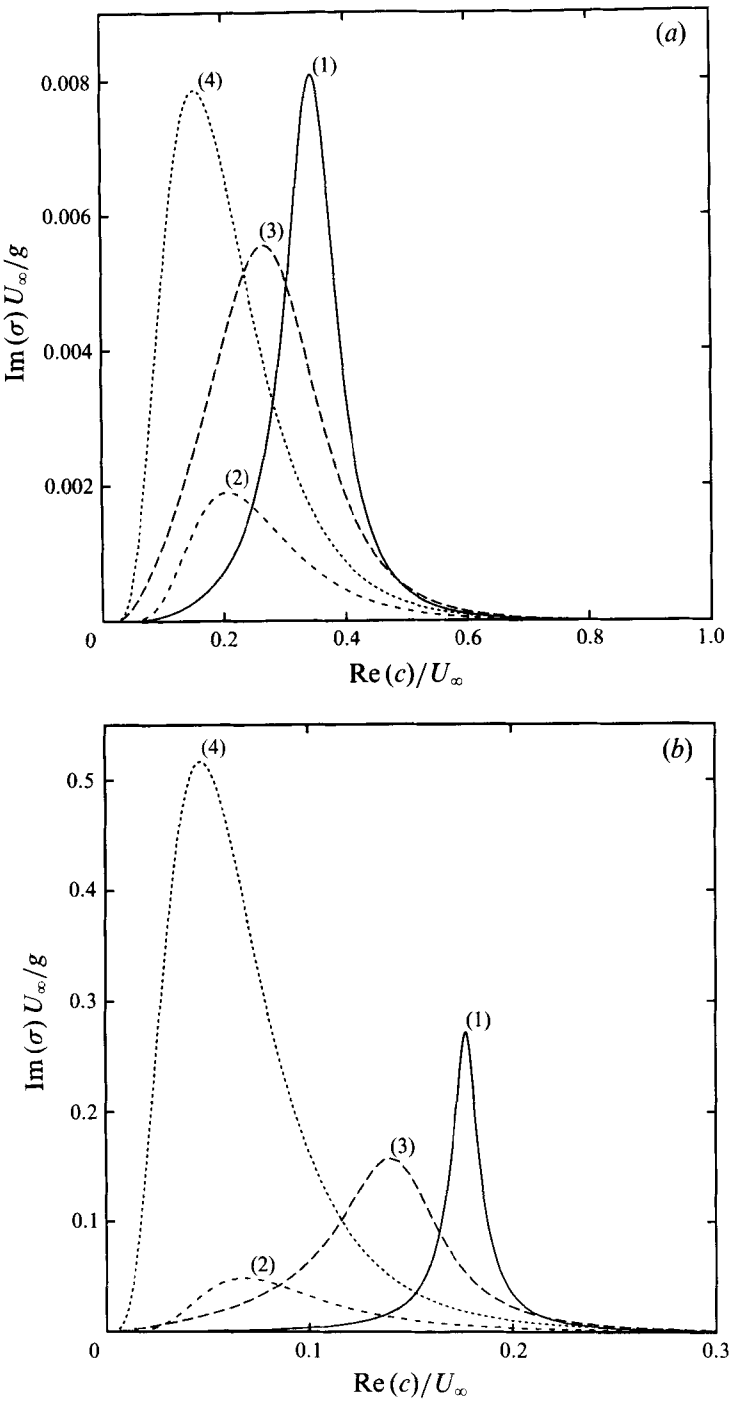

FIGURE 1. Growth rate against phase velocity as given by the Miles formula and the numerical computations for the exponential and error function profiles. Curve (1), numerics, error function profile; (2), Miles formula, error function profile; (3), numerics, exponential profile; (4), Miles formula, exponential profile. (*a*) $\Delta g/U_\infty^2 = 0.1$, (*b*) $\Delta g/U_\infty^2 = 0.01$.

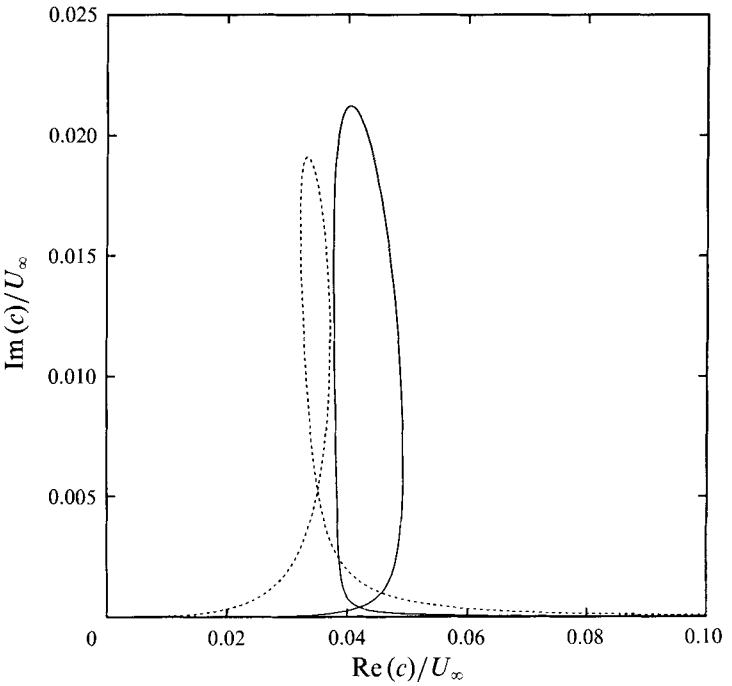

FIGURE 2. Imaginary part of wave speed against the phase velocity computed numerically for both profiles when $\Delta g/U_\infty^2 = 10^{-4}$. ——, Error function profile; – – –, exponential profile.

exponential profile at $\Delta g/U_\infty^2 = 0.01$ the maximum growth rate ratio of the Miles formula to the numerics is approximately 3 whilst at $\Delta g/U_\infty^2 = 0.1$ it is approximately 1.5, and when $\Delta g/U_\infty^2$ exceeds a value of approximately 0.2 the numerical growth rates exceed the Miles growth rates. At $\Delta g/U_\infty^2 = 1$ the ratio of maximum growth rates has fallen to $\frac{1}{5}$ for the exponential profile and $\frac{1}{10}$ for the error function profile and both values continue to decrease with increasing $\Delta g/U_\infty^2$. Figure 1(*a*, *b*) also shows that at a fixed $\Delta g/U_\infty^2$ the most unstable modes arising from the Miles formula have lower phase velocities, and hence wavelengths, than those arising from the numerics. We find this to be true at all values of $\Delta g/U_\infty^2$.

Figure 2 shows plots of the imaginary part of the wave speed against the real part from the numerical computations when $\Delta g/U_\infty^2 = 10^{-4}$. Figure 3 shows the corresponding plots of wavelength against phase velocity, and a plot of wavelength as a function of phase velocity for gravity waves. Figures 2 and 3 show the change in character of the instability at small values of $\Delta g/U_\infty^2$; there is a band of wavelengths for which the phase velocity is approximately constant and in which $\mathrm{Im}\,(c)/U_\infty$ attains its maximum value over all wavelengths. Away from this band of wavelengths $\mathrm{Im}\,(c)/U_\infty$ decays rapidly and the phase velocity tends to c_w.

When $\Delta g/U_\infty^2$ is decreased further our numerical results show that the dominant phase velocity of the unstable modes tends to the Kelvin–Helmholtz phase velocity. Similarly, the peak value of $\mathrm{Im}\,(c)$ tends to $s^{\frac{1}{2}}U_\infty/(1+s)$, which is the maximum value of $\mathrm{Im}\,(c)$ from (3.2) (and occurs at zero wavelength when $\Delta g/U_\infty^2 = 0$).

The logarithmic profiles show a clearer relationship between the Miles formula and the numerical computations, namely that growth rates calculated from the Miles formula significantly exceed those of the numerical computation. The qualitative agreement between the two methods of calculation is good as shown by figure 4(*a*, *b*),

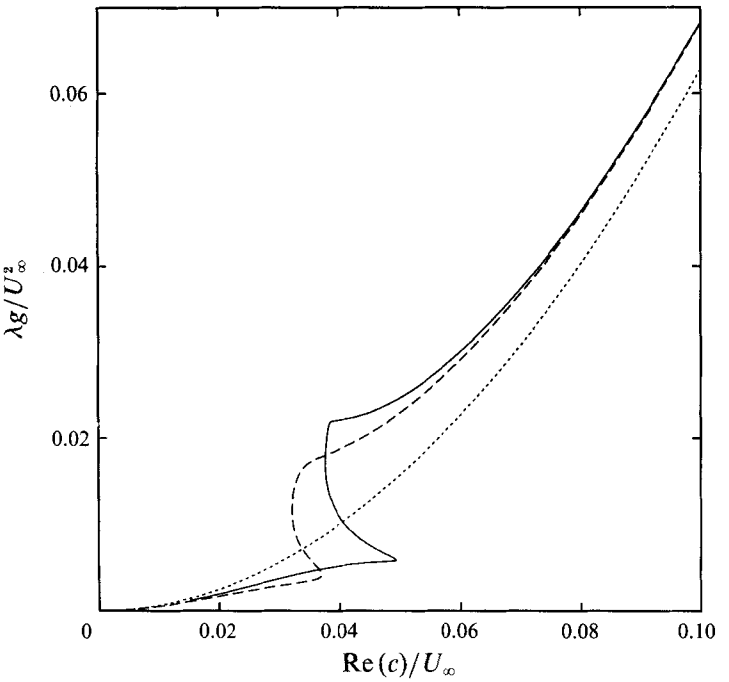

FIGURE 3. Wavelength against the phase velocity from the numerical computations and from the gravity wave dispersion relation $c = c_w$ when $\Delta g/U_\infty^2 = 10^{-4}$. ——, Error function profile; – – –, exponential profile; - - -, gravity waves.

which are plots of growth rate measured in s^{-1} against wavelength measured in m, for friction velocities of 9.7, 19, 30, 39 and 50 cm/s corresponding to wind speeds (according to the definition we have used) of 1.9, 3.8, 6, 7.8 and 10 m/s respectively.

The peak in growth rate that can be observed in all the plots occurs close to the wavelength at which the critical layer passes between the viscous sublayer and the constant-stress region and hence is not in the regime of validity of inviscid theory. The Miles–Benjamin theory and Valenzuela's computations indicate that when viscosity is included the growth rate peak occurs at wavelengths of order of a few centimetres for these friction velocities. Requiring that the critical layer is above the viscous sublayer gives an approximate bound on the wavelength for the validity of inviscid theory of $\lambda g/u_*^2 \gg 500$, where the velocity at the edge of the viscous sublayer has been taken to be $10u_*$.

We have also compared our numerical results with those in table 1 of Conte & Miles (1959). The difference in treatment of the air flow near the water surface between our stability analysis and Miles' theory prevents us from using Conte & Miles's logarithmic profile in our computations, so we have used the logarithmic profile given by equation (2.7c), with the parameters adjusted so that it is in agreement with Conte & Miles' profile for large y. We find that the results are in good agreement if the critical layer lies outside the viscous sublayer.

Our numerical results for the logarithmic profiles show that the growth rates of long waves for which the critical layer lies above the viscous sublayer are not sensitive to the details of the profile near the water surface. This is also a feature of Miles' formula, which depends only on the profile above the critical layer. As a consequence our results are also relevant to wind blowing over a surface on which waves have already

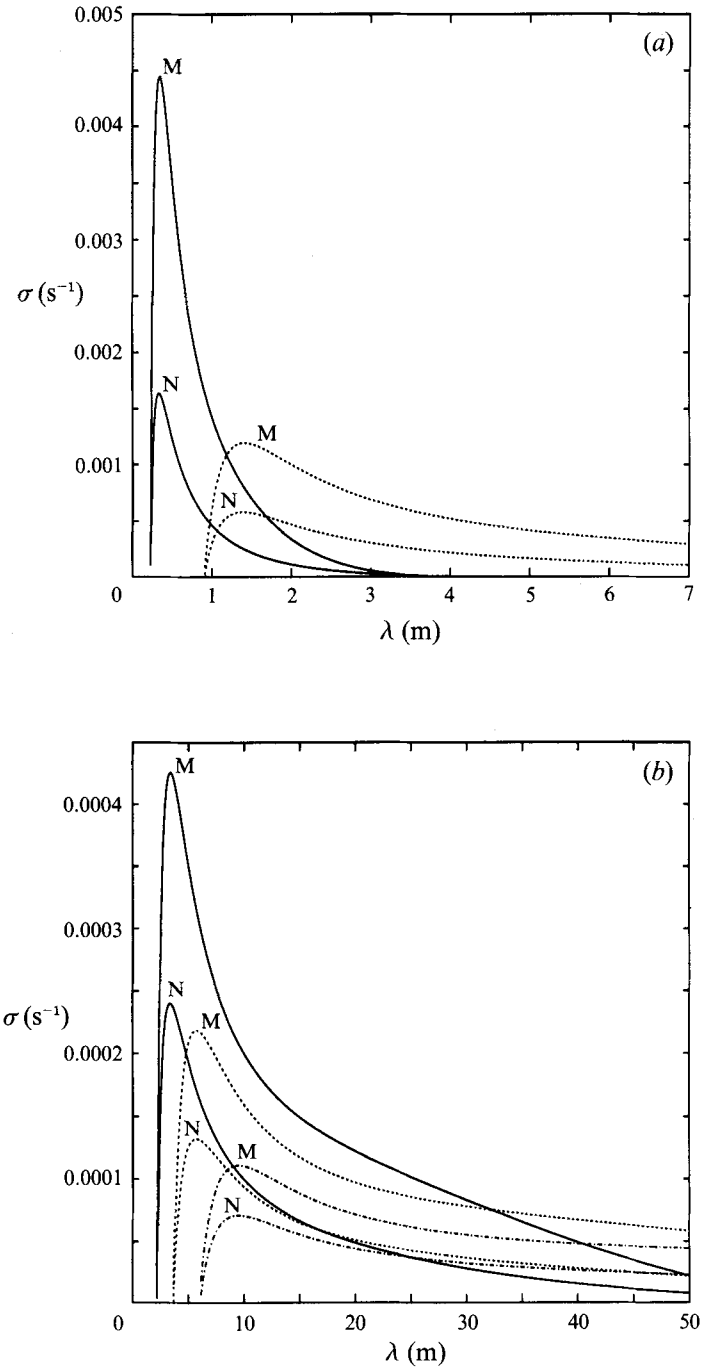

FIGURE 4. Growth rate against wavelength from the numerical computations (N) and from the Miles formula (M) for the 'lin-log' profile defined in (2.7*a*). (*a*) ——, $u_* = 9.7$ cm/s; – – –, $u_* = 19$ cm/s. (*b*) ——, $u_* = 30$ cm/s; - - -, $u_* = 39$ cm/s; – – – –, $u_* = 50$ cm/s.

developed, since above the waves the wind profile is logarithmic. (Miles 1957 reviews experimental work that supports this claim.) When there are waves present we cannot take into account the complicated form of the air flow near the water surface but this appears to be unnecessary. If the presence of waves is assumed to lead to a water surface with a roughness length, y_l the turbulent mean flow is given by $U(y) = (u_*/\kappa)\log(y/y_l)$ for $y > y_l$ and $y_1 \gg y_l$, where y_1 is the viscous sublayer thickness (Townsend 1976). Comparison with the smooth surface profiles for $y \gg y_1$ suggests that the influence of the presence of waves can be modelled by reducing the roughness constant A in (2.7). Reducing A leads to generally reduced growth rates but produces no qualitative changes to figure 4(a, b).

These observations suggest that if a wind starts to blow over initially still water the most rapidly growing waves will be short waves produced by the Miles–Benhamin mechanism. These waves will quickly equilibrate but the Miles mechanism will continue to act to produce longer waves.

4. Conclusions

An investigation of water-wave generation by the wind in which Miles' (1957) growth rate formula has been compared with numerical solutions of the Rayleigh equation has shown that growth rates are extremely sensitive to changes in the air velocity profile for laminar-type profiles but less so for the more physically relevant logarithmic-type profiles. In the latter case we observed good qualitative agreement between growth rates computed by the Miles formula and the numerical computations, but found that the Miles formula overestimated growth rates by a factor of approximately two. However, we found good agreement with the numerical computations of Conte & Miles (1959).

In the highly sheared limit the laminar profiles were shown to retrieve the Kelvin–Helmholtz instability of a vortex sheet.

We would like to thank one of the referees for suggesting significant improvements to the paper, and John W. Miles for his comments. Partial support by the Office of Naval Research (Grant N000-14-89-J-1164) is gratefully acknowledged.

Appendix A. Extension of the semicircle theorem and Squire's theorem

A.1. *The semicircle theorem*

Following Howard (1961) and Yih (1972) a new dependent variable $F = \phi/W$, where $W = U - c$, is introduced into the boundary value problem (2.4), which after substitution becomes

$$(W^2F')' - k^2W^2F = 0, \tag{A 1a}$$

$$[\rho(W^2F' - g)]_{\mathrm{w}}^{\mathrm{a}} = 0 \quad \text{on} \quad y = 0, \tag{A 1b}$$

$$F \to 0 \quad \text{as} \quad y \to \pm\infty. \tag{A 1c}$$

Multiplying (A 1a) by ρ_{w}, integrating from $-\infty$ to 0, performing an integration by parts, and then adding the resulting equation to its counterpart obtained by carrying out the analagous procedure on $(0, \infty)$ yields

$$\left(\rho_{\mathrm{w}}\int_{-\infty}^{0} \mathrm{d}y + \rho_{\mathrm{a}}\int_{0}^{\infty} \mathrm{d}y\right) W^2Q - ((\rho_{\mathrm{w}} - \rho_{\mathrm{a}})\, g)|F(0)|^2 = 0, \tag{A 2}$$

where use has been made of (A 1*b*) and (A 1*c*), and $Q = |F'|^2 + k^2|F|^2$. The imaginary part of (A 2) is

$$c_i\left(\rho_w \int_{-\infty}^{0} dy + \rho_a \int_{0}^{\infty} dy\right)(U - c_r)\, Q = 0, \tag{A 3}$$

from which it can be seen that a necessary condition for instability is $c_r \in (U_{min}, U_{max})$, where U_{min} and U_{max} are respectively the minimum and maximum values of U over both water and air. Taking the real part of (A 2) gives

$$\left(\rho_w \int_{-\infty}^{0} dy + \rho_a \int_{0}^{\infty} dy\right)((U - c_r)^2 - c_i^2)\, Q = ((\rho_w - \rho_a)\, g)|F(0)|^2. \tag{A 4}$$

If c_i is non-zero then (A 3) can be multiplied by c_r/c_i and added to (A 4) to yield

$$\left(\rho_w \int_{-\infty}^{0} dy + \rho_a \int_{0}^{\infty} dy\right)(U^2 - c_r^2 - c_i^2)\, Q \geqslant 0, \tag{A 5}$$

where the inequality sign follows from the right-hand side of (A 4) being positive. By noting that

$$\left(\rho_w \int_{-\infty}^{0} dy + \rho_a \int_{0}^{\infty} dy\right)(U^2 - (a+b)\, U + ab)\, Q \leqslant 0, \tag{A 6}$$

where $a = U_{min}$ and $b = U_{max}$, and using (A 3) and (A 5) to eliminate U from (A 6) it follows that

$$\left(\rho_w \int_{-\infty}^{0} dy + \rho_a \int_{0}^{\infty} dy\right)(c_r^2 + c_i^2 - (a+b)\, c_r + ab)\, Q \leqslant 0, \tag{A 7}$$

and hence

$$(c_r - \tfrac{1}{2}(a+b))^2 + c_i^2 \leqslant \tfrac{1}{2}(b-a)^2, \tag{A 8}$$

which is the semicircle theorem.

A.2. *Squire's theorem*

Consider three-dimensional disturbances proportional to $e^{i(\alpha x + \gamma z - \sigma t)}$, where the coordinate system is the extension to three dimensions of the system described in §2. The standard form of Squire's Transformation, described in Drazin & Reid (1981), relates the three-dimensional disturbance to an associated two-dimensional disturbance via

$$\hat{\alpha} = (\alpha^2 + \gamma^2)^{\frac{1}{2}}, \quad \hat{u} = \frac{\alpha u + \gamma w}{\hat{\alpha}}, \quad \hat{v} = v, \quad \hat{p} = \frac{\hat{\alpha} p}{\alpha}, \quad \hat{\sigma} = \frac{\sigma \hat{\alpha}}{\alpha}, \tag{A 9a–e}$$

where quantities in the associated two-dimensional problem are indicated by a 'hat' and u, v and w are the velocity components once the exponential dependence has been factored out. The transformation is extended to include the free boundary conditions (2.3*d*) and (2.3*e*) by putting

$$\hat{a} = \alpha a/\hat{\alpha}, \quad \hat{g} = (\hat{\alpha}/\alpha)^2\, g, \tag{A 10a, b}$$

where a is the wave amplitude, defined below (2.3), and g is the acceleration due to gravity. The transformation allows the growth rate for a three-dimensional disturbance to be computed from the growth rate for an associated two-dimensional disturbance.

For the laminar velocity profiles considered in this paper the parameter dependence of the growth rate of two-dimensional disturbances can be written as

$$\sigma_{2D}\, U_\infty / g = F(kU_\infty^2/g, \Delta g/U_\infty^2, \rho_a/\rho_w), \tag{A 11}$$

where k is the wavenumber in the x-direction. Hence, by applying the above transformation, the growth rate of the three-dimensional disturbance is given by

$$\sigma_{3D}\, U_\infty/g = (\hat{\alpha}/\alpha)\, F((\alpha/\hat{\alpha})^2\, U_\infty^2\, \hat{\alpha}/g, (\hat{\alpha}/\alpha)^2\, \Delta g/U_\infty^2, \rho_a/\rho_w). \tag{A 12}$$

We wish to compare the growth rate of the three-dimensional disturbance with those of two-dimensional disturbances under the influence of the same gravity and velocity profile. Equation (A 12) shows that the three-dimensional disturbance is equivalent to a two-dimensional disturbance at an increased value of Δ with g and U_∞ held fixed. Our calculations show that the maximum value over all wavenumbers of the function F decreases sufficiently rapidly with increasing $\Delta g/U_\infty^2$ that, despite the factor of $\hat{\alpha}/\alpha$, the growth rate of the three-dimensional disturbance is less than the maximum growth rate for two-dimensional disturbances. This means that for fixed gravity and velocity profile the most unstable disturbance is two-dimensional and the theorem is verified.

For the logarithmic profiles $\Delta g/U_\infty^2$ is replaced by $g\nu_a/U_\infty^3$ in (A 11) and $(\hat{\alpha}/\alpha)^2\, \Delta g/U_\infty^2$ is replaced by $(\hat{\alpha}/\alpha)^2\, \nu_a g/U_\infty^3$ in (A 12). However, in this case the maximum value of F does not decrease with increasing $\nu_a g/U_\infty^3$ (the dependence of F on $\nu_a g/U_\infty^3$ is qualitatively the same as the dependence of the dimensional growth rates on $1/u_*$, shown by figure 4) and hence the theorem does not follow.

Both the extension of the semicircle theorem and Squire's transformation and theorem can be modified to include surface tension without difficulty; the work of Yih and Morland *et al.*, which includes surface tension, demonstrates how it would be introduced into the derivations above.

Appendix B. Analytical integration for the exponential profile

By John Miles
IGPP, UCSD, 9500 Gilman Drive, La Jolla, CA 92093–0225, USA

It appears to be worth recording that the analytical solution of the Rayleigh equation (2.4a) for the exponential profile (2.6a) yields the exact solution (Hughes & Reid 1965)

$$\phi = \phi_c e^{-k(y-y_c)} f(t), \quad f(t) = \frac{F(p,q;r;t)}{F(p,q;r;1)}, \quad t = \frac{U_\infty - U}{U_\infty - c}, \tag{B 1a–c}$$

where

$$p = \alpha + (1+\alpha^2)^{\frac{1}{2}}, \quad q = \alpha - (1+\alpha^2)^{\frac{1}{2}}, \quad r = 1+2\alpha, \quad \alpha \equiv \tfrac{1}{2}k\Delta, \tag{B 2a–d}$$

F is a hypergeometric function, $y = (0, y_c, \infty)$ map to $t = (1+\epsilon, 1, 0)$ and

$$\epsilon \equiv \frac{c}{U_\infty - c}, \quad \frac{c}{U_\infty} = \frac{\epsilon}{1+\epsilon}. \tag{B 3a, b}$$

The expansion of $f(1+\epsilon)$ about $\epsilon = 0$ through the analytical continuation of $f(t)$ into $t > 1$ with $\arg(1-t) = -\pi$ for $t > 1$ (since $\operatorname{Im} y_c > 0$) yields

$$f(1+\epsilon) = 1 + \epsilon \sum_{n=0}^{\infty} \frac{a_n(-\epsilon)^n}{(n+1)!}(\log\epsilon - i\pi + h_n), \tag{B 4}$$

$$a_n = \frac{\Gamma(p+1+n)\Gamma(q+1+n)}{\Gamma(p+1)\Gamma(q+1)\Gamma(n+1)} = \left(2\alpha + \frac{n^2-1}{n}\right)a_{n-1}, \tag{B 5}$$

$$h_n = \psi(p+1+n) + \psi(q+1+n) - \psi(n+1) - \psi(n+2), \tag{B 6}$$

and ψ is the logarithmic derivative of the gamma function. Substituting (B 4) into (B 1 *a*) and letting $\epsilon \downarrow 0$ with $\alpha = O(1)$, we obtain

$$\phi_0/\phi_c = (1+\epsilon)^\alpha[1+\epsilon(1-\alpha\epsilon)(\ln\epsilon - i\pi + h_0) - (1-\tfrac{1}{2}\alpha)\epsilon^2 + O(\epsilon^3 \ln\epsilon)]. \tag{B 7}$$

If both α and ϵ are small,

$$\phi_0/\phi_c = 1 - \epsilon/\alpha + \epsilon(\ln\epsilon - \tfrac{1}{2} - i\pi - \epsilon^2 + 3.040\alpha\epsilon + \tfrac{1}{2}\epsilon^3 - 1.904\alpha^2\epsilon + \ldots. \tag{B 8}$$

The substitution of (B 8) into

$$\sigma = -\tfrac{1}{2}\pi sc\left(\frac{U_c''}{U_c'}\right)\left|\frac{\phi_c}{\phi_0}\right|^2 \tag{B 9}$$

for the exponential growth rate (Miles 1957) yields results in agreement with figure 1 (*a*, *b*) above.

Turning to the limit $\alpha \uparrow \infty$, we expand the gamma functions in

$$f(t) = -\sum_{n=0}^{\infty} \frac{\Gamma(p+n)\Gamma(q+n)}{\Gamma(r+n)\Gamma(1+n)} t^n \tag{B 10}$$

in inverse powers of α and invoke $\psi(z) \sim \log z$ to obtain

$$f(t) = 1 + \frac{1}{2\alpha}\left[\psi(2\alpha) - \psi(1) - \sum_{n=1}^{\infty}\frac{t^n}{n}\right] + O(\alpha^{-2}) \tag{B 11 a}$$

$$= 1 + \frac{1}{2\alpha}\left\{\log[2\alpha(1-t)] + \gamma\right\} + O(\alpha^{-2}), \tag{B 11 b}$$

where γ is Euler's constant. Substituting (B 11 *b*) into (B 1 *a*) and setting $t = 1+\epsilon$, we obtain

$$\frac{\phi_0}{\phi_c} = (1+\epsilon)^\alpha\left\{1 + \frac{1}{2\alpha}\left[\ln(2\alpha\epsilon) - i\pi + \gamma\right] + O(\alpha^{-2})\right\} \quad (\alpha \uparrow \infty). \tag{B 12}$$

This work was supported in part by the Division of Ocean Sciences of the National Science Foundation, NSF Grant OCE92-16397 and by the Office of Naval Research N00014-92-J-1171.

REFERENCES

AKYLAS, T. R. 1982 A nonlinear theory for the generation of water waves by wind. *Stud. Appl. Maths* **67**, 1–24.

BARNETT, T. P. & WILKERSON, J. C. 1967 On the generation of ocean wind waves as inferred from airborne radar measurements of fetch-limited spectra. *J. Mar. Res.* **25**, 292–321.

BENJAMIN, T. B. 1959 Shearing flow over a wavy boundary. *J. Fluid Mech.* **6**, 161–205.

CHANDRASEKHAR, S. 1970 *Hydrodynamic and Hydromagnetic Stability*. Oxford University Press.

CONTE, S. D. & MILES, J. W. 1959 On the numerical integration of the Orr–Sommerfeld equation. *J. Soc. Indust. Appl. Maths* **7**, 361–366.

DOBSON, F. W. 1971 Measurements of atmospheric pressure on wind-generated sea waves. *J. Fluid Mech.* **48**, 91–127.

DRAZIN, P. G. & REID, W. H. 1981 *Hydrodynamic Stability*. Cambridge University Press.

DUIN, C. A. VAN & JANSSEN, A. E. M. 1992 An analytic model of the generation of surface gravity waves by turbulent air flow. *J. Fluid Mech.* **236**, 197–215.

ELLIOTT, J. A. 1972 Microscale pressure fluctuations near waves being generated by the wind. *J. Fluid Mech.* **54**, 427–448.

GASTEL, K. VAN, JANSSEN, P. A. E. M. & KAMEN, G. J. 1985 On phase velocity and growth rate of wind-induced gravity–capillary waves. *J. Fluid Mech.* **161**, 199–216.

HASSELMAN, D. & BÖSENBERG, J. 1991 Field measurements of wave-induced pressure over wind-sea and swell. *J. Fluid Mech.* **230**, 391–428.

HOWARD, L. N. 1961 Note on a paper of John W. Miles. *J. Fluid Mech.* **10**, 509–512.

HUGHES, T. H. & REID, W. H. 1965 On the stability of the asymptotic suction boundary-layer profile. *J. Fluid Mech.* **23**, 715–735.

KAHMA, K. K. & DONELAN, M. A. 1988 A laboratory study of the minimum wind speed for wind wave generation. *J. Fluid Mech.* **192**, 339–364.

LIGHTHILL, M. J. 1962 Physical interpretation of the mathematical theory of wave generation by wind. *J. Fluid Mech.* **14**, 385–398.

LONG, R. B. 1980 A parametrical model for the vertical structure of the induced atmospheric pressure field above a spectrum of surface gravity waves. *J. Fluid Mech.* **99**, 163–183.

MAKIN, V. K. 1988 Numerical results on the structure of the sea wave-induced pressure field in the atmosphere. *Morskoy Gidofizichesky Zh.*, No. 2, 50–54.

MILES, J. W. 1957 On the generation of surface waves by shear flows. *J. Fluid Mech.* **3**, 185–204.

MILES, J. W. 1959 On the generation of surface waves by shear flows. Part 2. *J. Fluid Mech.* **6**, 569–582.

MILES, J. W. 1962*a* A note on the inviscid Orr–Sommerfeld equation. *J. Fluid Mech.* **13**, 427–432.

MILES, J. W. 1962*b* On the generation of surface waves by shear flows. Part 4. *J. Fluid Mech.* **13**, 433–448.

MORLAND, L. C., SAFFMAN, P. G. & YUEN, H. C. 1991 Waves generated by shear layer instabilities. *Proc. R. Soc. Lond.* A **433**, 441–450.

SHEMDIN, O. H. 1972 Wind-generated current and phase speed of wind waves. *J. Phys. Oceanogr.* **2**, 411–419.

SNYDER, R. L. 1974 A field study of wave-induced pressure fluctuations above surface gravity waves. *J. Mar. Res.* **32**, 497–529.

SNYDER, R. L. & COX, C. S. 1966 A field study of the wind generation of ocean waves. *J. Mar. Res.* **24**, 141–178.

SNYDER, R. L., DOBSON, F. W., ELLIOTT, J. A. & LONG, R. B. 1981 Array measurements of atmospheric pressure fluctuations above surface gravity waves. *J. Fluid Mech.* **102**, 1–59.

SQUIRE, H. B. 1933 On the stability of three-dimensional disturbances of viscous flow between parallel walls. *Proc. R. Soc. Lond.* A **142**, 621–628.

TOWNSEND, A. A. 1976 *The Structure of Turbulent Shear Flow*, 2nd edn. Cambridge University Press.

VALENZUELA, G. R. 1976 The growth of gravity–capillary waves in a coupled shear flow. *J. Fluid Mech.* **76**, 229–250.

YIH, C. S. 1972 Surface waves in flowing water. *J. Fluid Mech.* **51**, 209–220.